

Voids and overdensities of coupled Dark Energy

Roberto Mainini

Institute of Theoretical Astrophysics, University of Oslo, Box 1029, 0315 Oslo,
Norway

Abstract. We investigate the clustering properties of dynamical Dark Energy even in association of a possible coupling between Dark Energy and Dark Matter. We find that within matter inhomogeneities, Dark Energy might form voids as well as overdensity depending on how its background energy density evolves. Consequently and contrarily to what expected, Dark Energy fluctuations are found to be slightly suppressed if a coupling with Dark Matter is permitted. When considering density contrasts and scales typical of superclusters, voids and supervoids, perturbations amplitudes range from $|\delta_\phi| \sim \mathcal{O}(10^{-6})$ to $|\delta_\phi| \sim \mathcal{O}(10^{-4})$ indicating an almost homogeneous Dark Energy component.

PACS numbers:

1. Introduction

Several observations made over the recent years, related to a large extension to Large Scale Structures (LSS) and anisotropies of the Cosmic Microwave Background (CMB) as well as the magnitude–redshift relation for type Ia Supernovae [1], have given us a convincing picture of the energy and matter density in the Universe.

Baryonic matter accounts for no more than 30% of the mass in galaxy clusters while the existence of a large clustered component of Dark Matter (DM) seems now firmly established, although its nature is still unknown. However, they contribute to the total energy density of the Universe with only a few percent and about 25% respectively.

No more than another few percent could be accounted for by massive neutrinos, but only in the most favorable, but unlikely case. According to [2] the total mass of neutrinos cannot exceed the limit of $1.43 eV$ (see, however, [3] for a recent analysis on neutrino mass limits in coupled dark energy models). A very small part (10^{-4}) of the total energy density is due to massless neutrinos and CMB radiation.

The model suggested by observations is only viable if the remaining 75% is ascribed to the so–called Dark Energy (DE) responsible for the present day cosmic acceleration.

Although strongly indicated by the observations, the existence of DE is even more puzzling than DM. It can be identified with a cosmological constant or with a yet unknown dynamical component with negative pressure. On the other hand, its manifestation can be interpreted as a geometrical property of the gravity on large scales resulting from a failure of General Relativity (GR) on those scales (see [4] for a review).

Within the context of GR, as an alternative to the cosmological constant, DE is usually described as a self–interacting scalar field or a cosmic fluid with negative pressure (see [5] and references therein). It is usually assumed that density perturbations of DE play a negligible role in the structure formation because of its very small mass $\sim H$ (H being the Hubble parameter). Accordingly, perturbations should appear only on very large scales (>100 Mpc) and are bound to be linear so that rates of structure formation and their growth are influenced by DE only through the overall cosmic expansion [6].

Nevertheless, this assertion remains questionable and its validity has been subject to recent debate. Then, the key question is whether DE actively participates in the clustering and virialization processes possibly developing non–linearity on relevant scales. Some attempts to solve the problem have been done in [7, 8, 9, 10], sometimes adopting a phenomenological approach parametrizing the observables associated with DE clustering or in the context of coupled DE and other non–trivial DE models where clustering is expected to be more probable.

An intriguing result was obtained by Dutta & Maor [9]. They numerically studied the clustering of DE within matter overdensities showing that DE tends to form underdensities or voids in response to the gravitationally collapsing matter (similarly, DE overdensities are expected in correspondence of matter underdensities). On supercluster scales they found $|\delta_\phi| \sim \mathcal{O}(10^{-2})$ when $\delta_m \sim \mathcal{O}(1)$ which could be relevant to observations (δ_m and δ_ϕ being the density contrast of matter and DE

respectively). However, their analysis was limited to linear spherical perturbations and the simplest class of DE models in which DE is ascribed to a light scalar field ϕ slowly-rolling down its potential $V(\phi)$, minimally coupled to matter and gravity.

A similar problem was investigated by Mota et al [10] with a different approach providing an analytical approximation for δ_ϕ valid both in linear and nonlinear regime ($\delta_m > \mathcal{O}(1)$) in uncoupled scalar field DE models. However, in spite of the qualitative agreement of their results with those of Dutta & Maor [9], they found $|\delta_\phi| \sim \mathcal{O}(10^{-5})$ when the same linear scales are considered.

In the present paper we extend the analysis of Dutta & Maor [9] taking into account a possible coupling between DM and DE and considering a wider class of DE tracking potentials. Then, we numerically study DE clustering on those scales for which $\delta_m \sim \mathcal{O}(1)$ today, i.e. supercluster, void and supervoid scales, and show that, coupled as well as uncoupled DE develops inhomogeneities which amplitudes are consistent with the findings of Mota et al [10]. Formation of DE voids (overdensities) is however related to how the background energy density of DE evolves and not only to the presence of matter overdensities (underdensities) as claimed in the previous works. It is also shown that, as expected, the growth of matter fluctuations is suppressed as soon as DE starts to drive the cosmic acceleration while $\delta_\phi \rightarrow 0$ as DE, in the models here considered, asymptotically approaches a cosmological constant.

The plan of the paper is as follows: in Section 2 we describe our model and give the linearized equations for matter, DE and metric perturbations which are derived in Appendix A. Numerical results concerning perturbation evolution are presented and discussed in Section 3. We summarize and conclude in Section 4.

2. The model

The essential feature of a scalar field ϕ , in order to yield DE and drive the cosmic acceleration, is its self-interaction through a potential $V(\phi)$.

In addition to self-interaction, a scalar field can in principle be coupled to any other field present in nature. Couplings to ordinary particles are strongly constrained by observational limits on violations of the equivalence principle but limits on the DM coupling are looser (constraints on coupling for specific models were obtained in [11, 12] from CMB, N-body simulations and matter power spectrum analysis). If present, DM coupling could have a relevant role in the cosmological evolution affecting not only the overall cosmic expansion but also modifying the DM particles dynamics with relevant consequences for the growth of the density perturbations in both the linear and nonlinear regime (e.g., on halo density profiles, mass function and its evolution) [11, 13, 14]. Here we consider one of the most popular models where a coupling between DM and DE is present, namely coupled DE [13] (for different DE-matter interactions see [15]).

According to general covariance, the sum of the individual stress energy tensors $T_{(i)\nu}^\mu$ ($i = b, dm, \phi$) must be conserved so we can write:

$$\nabla_\mu T_{(b)\nu}^\mu = 0 \quad \nabla_\mu T_{(dm)\nu}^\mu = -CT_{(dm)} \nabla_\nu \phi \quad \nabla_\mu T_{(\phi)\nu}^\mu = CT_{(dm)} \nabla_\nu \phi \quad (1)$$

Here ∇_μ is the covariant derivative, $T_{(dm)}$ indicates the trace of the DM stress energy tensor and C is a constant which parametrizes the strength of the DM–DE interaction.

In a spacetime described by a metric $g_{\mu\nu}$ with signature $(-+++)$, the DE stress energy tensor takes the form:

$$T_{(\phi)\nu}^\mu = \partial^\mu \phi \partial_\nu \phi - \delta_\nu^\mu \left(\frac{1}{2} \partial_\sigma \phi \partial^\sigma \phi + V \right) \quad (2)$$

while baryons and DM are well described as non-relativistic pressureless perfect fluids with:

$$T_{(i)\nu}^\mu = \rho_i u_{(i)}^\mu u_{\nu(i)} \quad (3)$$

where ρ_i is the energy density of the component $i = b, dm$ and $u_{(i)}^\mu$ is its 4-velocity.

As we are interested in spherical perturbations around a spatially flat Friedmann–Robertson–Walker (FWR) background, only spherically symmetric spacetimes are considered for which the most general line element in comoving coordinates is:

$$ds^2 = -dt^2 + \mathcal{U}(t, r) dr^2 + \mathcal{V}(t, r) (d\theta^2 + \sin^2 \theta d\varphi^2) , \quad (4)$$

where $\mathcal{U}(t, r)$ and $\mathcal{V}(t, r)$ are general functions [16].

2.1. Background and perturbation equations

As usual, equations for background and perturbation evolution follow from (1) and Einstein's equations. In this Section we only state the full set of equations while their derivation is detailed in Appendix A. Working in the synchronous gauge, we redefine the metric functions as follows:

$$\begin{aligned} \mathcal{U}(t, r) &= a(t)^2 e^{2\zeta(t, r)} \\ \mathcal{V}(t, r) &= r^2 a(t)^2 e^{2\psi(t, r)} \end{aligned} \quad (5)$$

Here $a(t)$ is the scale factor of the homogeneous background while ζ and ψ represent deviations from homogeneity. In the following, however, metric perturbations will be described by $\chi = \dot{\zeta} + 2\dot{\psi}$, the only combination which is relevant to the equations of motion (see Appendix A for more details). We also decompose ϕ , ρ_{dm} and ρ_b as the sum of an unperturbed part, denoted by $\bar{}$, and a perturbed one:

$$\begin{aligned} \phi(t, r) &= \bar{\phi}(t) + \delta\phi(t, r) \\ \rho_{dm}(t, r) &= \bar{\rho}_{dm}(t) + \delta\rho_{dm}(t, r) \\ \rho_b(t, r) &= \bar{\rho}_b(t) + \delta\rho_b(t, r) \end{aligned} \quad (6)$$

and, for each component i , we define the density parameter $\Omega_i = \bar{\rho}_i / \rho_{cr}$, the density contrast $\delta_i = \delta\rho_i / \bar{\rho}_i$ and $\theta_i = \text{div } \mathbf{v}_i$ (ρ_{cr} and \mathbf{v}_i being the critical energy density and the coordinate velocity respectively). We assume perturbations to be small so that linear approximation applies. Further, only radial motions are considered, i.e. $|\mathbf{v}| = v^r = dr/d\tau$.

Hereafter we make use of conformal time τ related to cosmic time t via the equation $dt = a d\tau$. Derivatives with respect to τ are denoted with an overdot and the conformal Hubble function $\mathcal{H} = \dot{a}/a = aH$.

From (2), it is possible to work out the background energy density of DE, its pressure \bar{P}_ϕ , the corresponding perturbations as well as the radial velocity:

$$\begin{aligned}
 \bar{\rho}_\phi &= \frac{\dot{\bar{\phi}}^2}{2a^2} + \bar{V} & \delta\rho_\phi &= \frac{\dot{\bar{\phi}}\delta\dot{\bar{\phi}}}{a^2} + \bar{V}'\delta\phi \\
 \bar{P}_\phi &= \frac{\dot{\bar{\phi}}^2}{2a^2} - \bar{V} & \delta P_\phi &= \frac{\dot{\bar{\phi}}\delta\dot{\bar{\phi}}}{a^2} - \bar{V}'\delta\phi \\
 v_\phi^r &= \frac{\partial_r \delta\phi}{\dot{\bar{\phi}}}
 \end{aligned} \tag{7}$$

where $\bar{V} = V(\bar{\phi})$ and $'$ denotes the derivative with respect to $\bar{\phi}$.

With the above notation and definitions, the equations for background evolution read:

$$\begin{aligned}
 3\mathcal{H}^2 &= 8\pi G [\bar{\rho}_{dm} + \bar{\rho}_b + \bar{\rho}_\phi] a^2 \\
 \ddot{\bar{\phi}} + 2\mathcal{H}\dot{\bar{\phi}} + a^2\bar{V}' &= C\bar{\rho}_{dm}a^2 \\
 \dot{\bar{\rho}}_{dm} + 3\mathcal{H}\bar{\rho}_{dm} &= -C\bar{\rho}_{dm}\dot{\bar{\phi}} \\
 \dot{\bar{\rho}}_b + 3\mathcal{H}\bar{\rho}_b &= 0
 \end{aligned} \tag{8}$$

while linear perturbations evolve according to:

$$\begin{aligned}
 \ddot{\delta\phi} + 2\mathcal{H}\dot{\delta\phi} - \nabla^2\delta\phi + a^2\bar{V}''\delta\phi + \chi\dot{\bar{\phi}} &= C\delta_{dm}\bar{\rho}_{dm}a^2 \\
 \dot{\delta}_{dm} + \theta_{dm} + \chi &= -C\dot{\delta\phi} \\
 \dot{\theta}_{dm} + \mathcal{H}\theta_{dm} &= C\left(\dot{\bar{\phi}}\theta_{dm} + \nabla^2\delta\phi\right) \\
 \dot{\delta}_b + \theta_b + \chi &= 0 \\
 \dot{\theta}_b + \mathcal{H}\theta_b &= 0 \\
 \dot{\chi} + \mathcal{H}\chi - \frac{3}{2}\mathcal{H}^2 \left[\Omega_{dm}\delta_{dm} + \Omega_b\delta_b + \Omega_\phi \left(\delta_\phi + 3\frac{\delta P_\phi}{\bar{\rho}_\phi} \right) \right] &= 0
 \end{aligned} \tag{9}$$

Note that, in the absence of coupling, $C = 0$, DM particles and baryons follow the same dynamics and can be used to define the synchronous coordinates and therefore have zero peculiar velocity ($\theta_{dm} = \theta_b = 0$). θ_i 's equations are not needed anymore and the set of equations (8) and (9) then reduces to that given in Dutta & Maor [9].

On the other hand, as widely discussed in [13], coupling modifies the dynamics of DM particles and an equation for θ_{dm} is therefore needed: although $\theta_{dm} = 0$ initially, it can not remain null for all times because of the term $C\left(\nabla^2\delta\phi + \dot{\bar{\phi}}\theta_{dm}\right)$. As a consequence baryons and DM develop a bias b , i.e. $\delta_b = b\delta_{dm}$. Anyway, it is still possible to eliminate the variable θ_b reducing the number of equations by one.

It is also worth mentioning that, unlike the uncoupled case, in the presence of coupling, Universe goes through an evolutionary phase named ϕ -matter dominated era (ϕ MDE) just after matter-radiation equivalence. In this period the scalar field ϕ behaves as *stiff matter* ($P_\phi/\rho_\phi = 1$) having a non-negligible kinetic energy which dominates over the potential one. After this stage, the usual matter era follows before entering in the accelerated regime.

In order to perform a numerical integration, it is most convenient to work in the Fourier space. Setting $\theta_b = 0$, equations (9) then become:

$$\begin{aligned}
 \ddot{\delta}\phi_k + 2\mathcal{H}\dot{\delta}\phi_k + k^2\delta\phi_k + a^2\bar{V}''\delta\phi_k + \chi_k\dot{\bar{\phi}} &= C\delta_{dm,k}\bar{\rho}_{dm}a^2 \\
 \dot{\delta}_{dm,k} + \theta_{dm,k} + \chi_k &= -C\delta\dot{\phi}_k \\
 \dot{\theta}_{dm,k} + \mathcal{H}\theta_{dm,k} &= C\left(\dot{\bar{\phi}}\theta_{dm,k} - k^2\delta\phi_k\right) \\
 \dot{\delta}_{b,k} + \chi_k &= 0 \\
 \dot{\chi}_k + \mathcal{H}\chi_k - \frac{3}{2}\mathcal{H}^2\left[\Omega_{dm}\delta_{dm,k} + \Omega_b\delta_{b,k} + \Omega_\phi\left(\delta_{\phi,k} + 3\frac{\delta P_{\phi,k}}{\bar{\rho}_\phi}\right)\right] &= 0
 \end{aligned} \tag{10}$$

where the index k denotes the Fourier-components with wavenumber k .

After having numerically evolved the above equations, their solutions are then Fourier transformed back to the coordinate space.

2.2. Potential

The present analysis is based on the assumption that DE is a self-interacting scalar field ϕ . Two self-interaction potentials are considered [17]:

$$V(\phi) = \Lambda^{\alpha+4}/\phi^\alpha \quad RP \tag{11}$$

or

$$V(\phi) = (\Lambda^{\alpha+4}/\phi^\alpha) \exp(4\pi\frac{\phi^2}{m_p^2}) \quad SUGRA \tag{12}$$

($m_p = G^{-1/2}$ is the Planck mass) admitting tracker solutions and initially introduced to ease the fine tuning and coincidence problems. In the absence of DM-DE coupling, RP yields quite a slowly varying $w(a) = \bar{P}_\phi/\bar{\rho}_\phi$ state parameter. On the contrary, SUGRA yields a fastly varying $w(a)$. Although coupling causes a $w(a)$ behavior significantly different from the uncoupled case, one could again consider these potentials as examples of rapidly or slowly varying $w(a)$.

For any choice of the energy scale Λ and the positive parameter α , the above potentials yield a fixed Ω_ϕ . Here we prefer to use Λ and Ω_ϕ as free parameters; the related α value is then suitably fixed. Λ values are chosen according to the constraints given in [18].

The use of the above potentials also permit to verify the generality of the Dutta & Maor [9] results obtained for different ones, namely the mass potential $V = m^2\phi^2/2$ and the double exponential potential [19].

In both uncoupled and coupled cases, the above potentials admit a final de Sitter attractor ($\Omega_\phi = 1, w = -1$) toward which universe asymptotically evolves. The behavior of the scalar field in this last stage is however different in the two cases. In the SUGRA model, driven by damped oscillations, the field approaches the minimum of its potential rather than asymptotically approaching infinity as in the RP case. As we will see in the next section, perturbations reflect the same behaviors.

2.3. Initial conditions

As in Dutta & Maor [9], perturbations in baryons and DM are initially taken to be gaussian:

$$\delta_{dm}(\tau_i, r) = A(\tau_i)e^{-\frac{r^2}{\sigma^2}} \quad \delta_b(\tau_i, r) = b\delta_{dm}(\tau_i, r) \quad (13)$$

(here τ_i is some initial time in the matter era). The ratio between fluctuation amplitudes in baryon and DM is prescribed by linear theory [13]:

$$b \simeq \frac{3\Omega_{dm}}{3\gamma\Omega_{dm} + 4\beta\mu\sqrt{\Omega_k}} \quad (14)$$

where $\beta = \sqrt{3/16\pi m_p C}$ is the adimensional coupling parameter, $\mu = (\dot{\delta}_{dm}/\delta_{dm})/(\dot{a}/a)$, $\gamma = 1 + 4\beta^2/3$ and $\Omega_k = \dot{\phi}^2/2a^2\rho_{cr}$.

The initial perturbation amplitude $A(\tau_i)$ is chosen such that the mean value of the total matter density contrast $\delta = (\delta\rho_b + \delta\rho_{dm})/(\rho_b + \rho_{dm})$ within the comoving radius $R = \sigma$ at the present time τ_0 is:

$$|\bar{\delta}(r < R, \tau_0)| = \left| \frac{\int_0^R \delta(r, \tau_0) r^2 dr}{\int_0^R r^2 dr} \right| \sim 1 \quad (15)$$

when dealing with supercluster and voids scales ($\sim 10 - 25h^{-1}$ Mpc). Slightly smaller $|\bar{\delta}_m|$ will be considered for supervoid scales (see next section).

We assume the shape of matter perturbations to be only slightly affected during their evolution so that δ_{dm} and δ_b are still well approximated by a gaussian at τ_0 . We will see in the next section that this assumption is confirmed by numerical results. Thus, setting $\delta = N\delta_{dm} = NAe^{-\frac{r^2}{\sigma^2}}$ we have:

$$\bar{\delta}(r < R, \tau) = \frac{3}{2}NA \left[\frac{\sqrt{\pi}}{2} \frac{\sigma}{R} \text{erf} \left(\frac{R}{\sigma} \right) - e^{-\frac{R^2}{\sigma^2}} \right] \frac{\sigma^2}{R^2} \quad (16)$$

where $N = (b\Omega_b + \Omega_{dm})/(\Omega_b + \Omega_{dm})$. For $R = \sigma$ and $\tau = \tau_0$ it follows $A \sim 1.76/N$ when $\bar{\delta} \sim 1$.

Dutta & Maor [9] set the initial redshift to $z_i = 35$ assuming $\delta\phi, \dot{\delta}\phi = 0$. However, DE fluctuations would have evolved since the earlier stages of the Universe and, although small, they are expected to differ from zero at z_i being then in tracking regime. With their choice for the initial conditions, Dutta & Maor [9] find that, initially, DE has a weak tendency to collapse. However, this effect has to be understood as due to the fact that such initial values do not lie on the tracker solution of the perturbed scalar field equation. This is clearly illustrated in Figure 1 where the evolution of the density contrast at the center of a matter overdensity is plotted for different choices of the initial conditions. In the top panel we compare the behaviors of δ_ϕ when choosing $\delta\phi, \dot{\delta}\phi = 0$ at different initial redshifts, i.e. $z_i = 100, 500, 1000$. Notice the initial tendency of DE to cluster. However, for different choices of $\delta\phi$ and $\dot{\delta}\phi$ the initial behavior of δ_ϕ will be completely different. This is shown in the bottom panel, where we permit initial values to differ from zero. An inspection of the plots, shows that independently from the initial conditions chosen, after an initial transient period, δ_ϕ always settles on the same

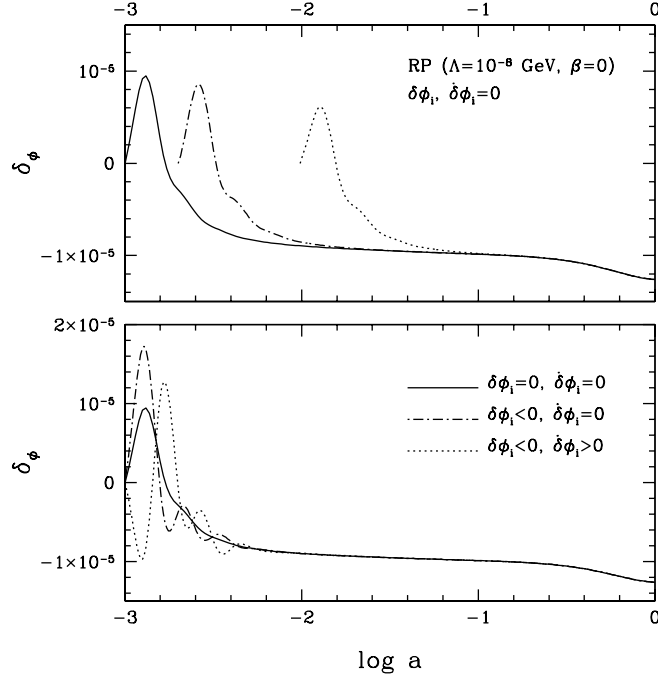


Figure 1. Evolution of the DE density contrast, δ_ϕ , at the center of a spherical matter overdensity for different initial conditions. In the top panel we set $\delta_\phi, \dot{\delta}_\phi = 0$ at different initial redshifts ($z_i = 100, 500, 1000$) while in the bottom panel we plot the behavior of δ_ϕ when the initial values of δ_ϕ and $\dot{\delta}_\phi$ differ from zero. Independently from the initial conditions chosen, after an initial transient period, δ_ϕ always settles on the same (tracker) solution.

(tracker) solution. Plots are given for a specific RP model but the same conclusions are reached when considering different cases.

Based on the above considerations, we choose initial conditions such that δ_ϕ arranges itself on the tracker solution already at $z = 100$ (e.g. $\delta_\phi, \dot{\delta}_\phi = 0, z_i = 1000$).

Finally, we set $\chi(\tau_i, r) = 0$ assuring that matter perturbations initially expand with the Hubble flow.

3. Results

In this section we present the results of numerical runs. In order to better understand the behavior of the perturbations around the present time, we stopped our runs at some time in the future. Results are then shown in the redshift range $100 < z < -0.99$ and, for $\sigma = 20h^{-1}$ Mpc if not otherwise specified. All models considered are spatially flat, have adimensional Hubble parameter $h = 0.70$, $\Omega_b = 0.046$ and $\Omega_{dm} = 0.234$.

Let us start first with the uncoupled case. Figure 2 compares the time evolution of the DE density contrast, δ_ϕ , at the center of matter overdensity ($r = 0$), in RP and SUGRA (uncoupled) cases. Both models present the same qualitative behavior

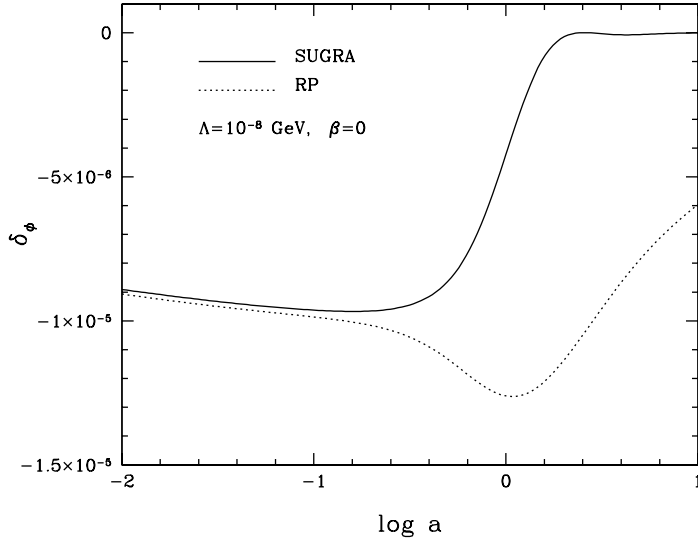


Figure 2. Evolution of the DE density contrast, δ_ϕ , at the center of a spherical matter overdensity in RP (dotted line) and SUGRA (solid line) uncoupled models. The comoving scale of the perturbation is $\sigma = 20h^{-1}$ Mpc and the mean matter density contrast within the radius $R = \sigma$ is $\bar{\delta} = 1$ at the present time.

until DE starts to dominate the cosmic expansion and ϕ approaches the Plack mass m_p . Differences in the late time behaviors are then to ascribe to the exponential term in (12) which dictates the late evolution of ϕ in SUGRA model as explained in the previous section.

Just as Dutta & Maor [9] and Mota et al [10] we find that DE tends to form voids in correspondence of matter overdensities obtaining $|\delta_\phi| \sim \mathcal{O}(10^{-5} - 10^{-6})$ in late matter era. While this is consistent with the findings of Mota et al [10], it does not agree with those reported by Dutta & Maor [9], i.e. $|\delta_\phi| \sim \mathcal{O}(10^{-2})$. Following the same arguments by Dutta & Maor [9], voids formation is understood as a 'drag effect' due to the slower expansion of the regions with matter overdensities. Matter collapse lowers the local value of H , reducing the Hubble damping to the scalar field. Therefore, in those regions, ϕ rolls down its potential slightly faster increasing its background value $\bar{\phi}$ and $\dot{\bar{\phi}}$ by the quantities $\delta\phi$ and $\dot{\delta}\phi$ respectively. Noticing that $\bar{\phi}, \dot{\bar{\phi}}, \delta\phi, \dot{\delta}\phi > 0$ while $\bar{V}' < 0$, a local void in DE, i.e. $\delta\rho_\phi = \delta\rho_V + \delta\rho_k < 0$, will form when the local variation in the potential energy density, $\delta\rho_V = \bar{V}'\delta\phi$, dominates over that in the kinetic energy density $\delta\rho_k = \dot{\bar{\phi}}\dot{\delta}\phi/a^2$.

This is exactly what happens in the uncoupled models here considered during the

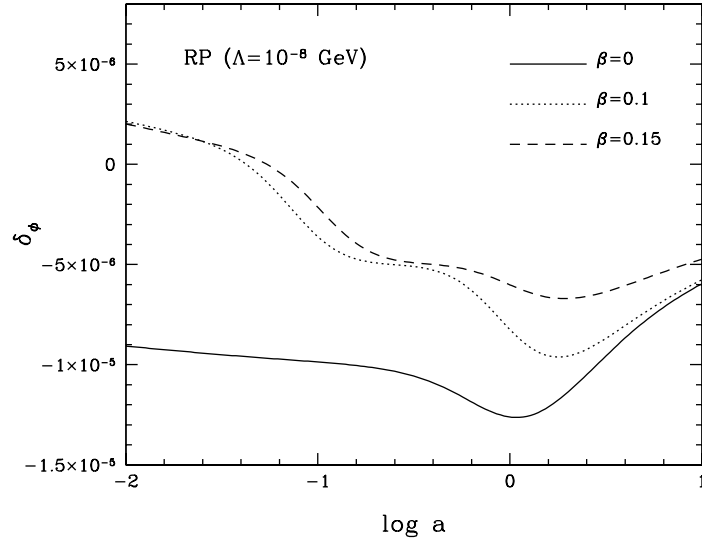


Figure 3. Evolution of the DE density contrast, δ_ϕ , at the center of a spherical matter overdensity for different values of the coupling parameter β in RP models. The comoving scale of the perturbation is $\sigma = 20h^{-1}$ Mpc and the mean matter density contrast within the radius $R = \sigma$ is $\bar{\delta} = 1$ at the present time.

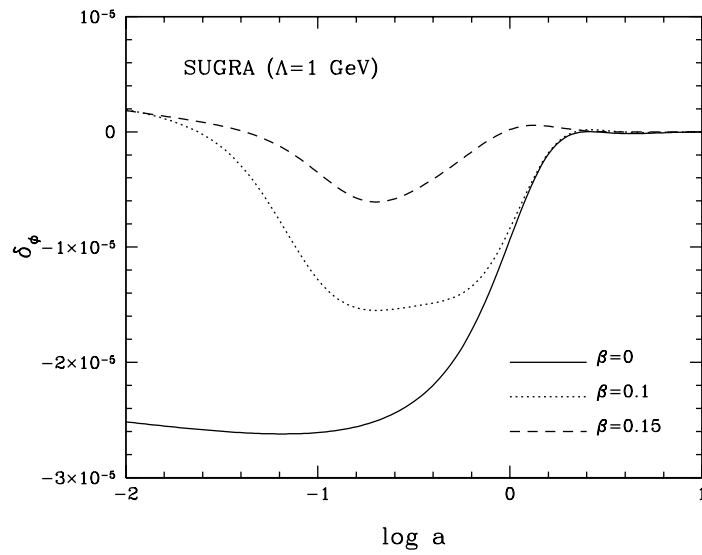


Figure 4. Same as Figure 3 but using the SUGRA potential.

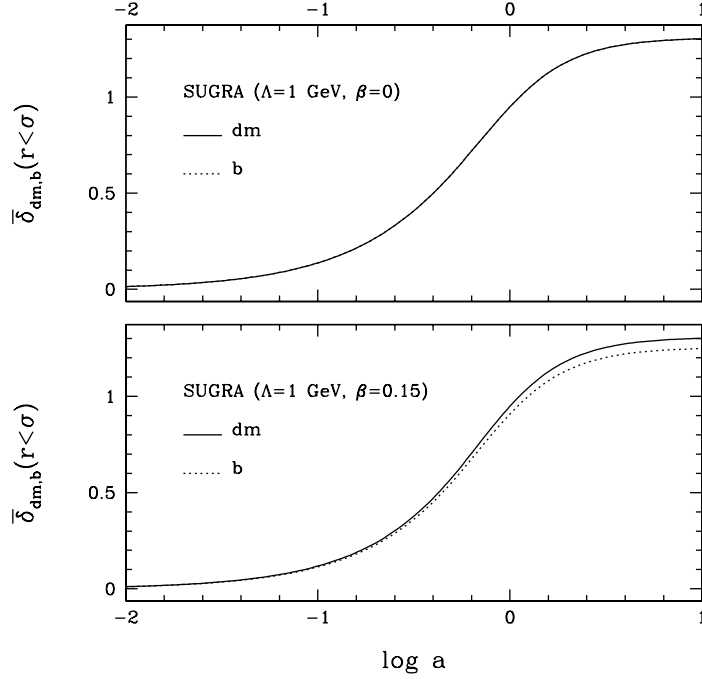


Figure 5. *Top panel:* evolution of the mean density contrast, $\bar{\delta}_{dm,b}$ of DM (solid line) and baryons (dotted line) in the uncoupled SUGRA case. *Bottom panel:* same as top panel but in the coupled case. Notice how the coupling introduces a bias between DM and baryons causing fluctuations to grow at different rates. Plots are given for the comoving scale $\sigma = 20h^{-1}$ Mpc. The mean matter density contrast within the radius $R = \sigma$ is $\bar{\delta} = 1$ at the present time.

tracking regime in matter era. In fact, in order to have $|\delta\rho_V| > |\delta\rho_k|$ it must be:

$$\left| \frac{\delta\rho_V}{\delta\rho_k} \right| = \frac{\alpha \bar{\rho}_V}{2 \bar{\rho}_k} = \frac{\alpha}{2} \frac{1-w}{1+w} > 1 \quad (17)$$

where $\bar{\rho}_k = \dot{\bar{\phi}}^2/2a^2$ and $\bar{\rho}_V = \bar{V}$ are the kinetic and potential background energy densities of DE and we made use of the tracker solution $\bar{\phi} \propto \delta\phi \propto \tau^{6/\alpha+2}$. Noticing that in this regime we also have $w = -2/(\alpha+2)$, relation (17) is always satisfied requiring $\alpha > 0$.

The above arguments, however, show that in general a local excess of matter is necessary but not sufficient to assure the formation of a corresponding DE underdensity, the mechanism being related to the behavior of the background energy density of DE, e.g. in our specific case, through the relation:

$$\bar{\rho}_V > \frac{2}{\alpha} \bar{\rho}_k \quad (18)$$

Therefore, some differences in the evolution of δ_ϕ arise when DM–DE coupling is considered, mainly due to the presence of the ϕ MDE. As long as the ϕ MDE holds, the kinetic energy of DE dominates over its potential energy invalidating (18) and yielding a positive δ_ϕ . This is shown in Figures 3 and 4 which plot the time evolution of δ_ϕ for different values of the coupling parameter β in RP and SUGRA cases.

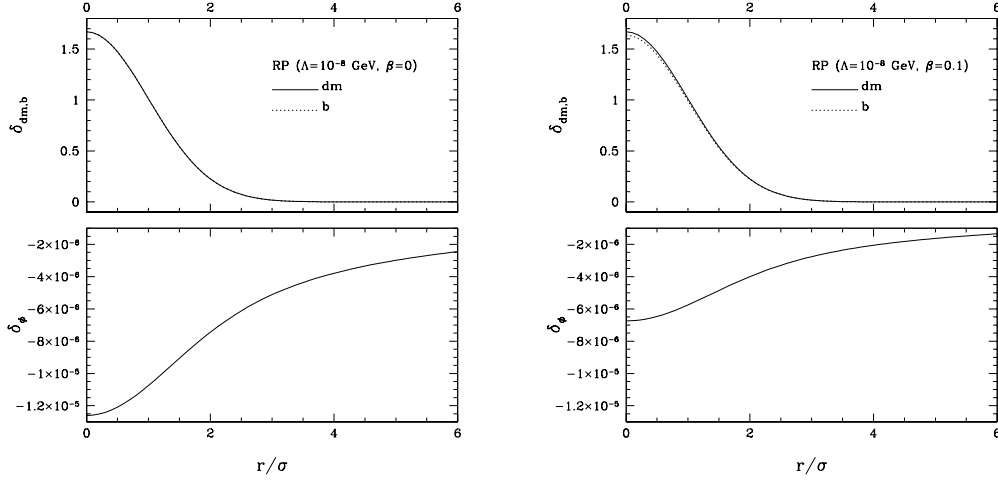


Figure 6. Density profiles of DM, baryons (top) and DE (bottom) at the present time in the uncoupled (left) and coupled (right) RP model. Plots are given for the comoving scale $\sigma = 20h^{-1}$ Mpc. The mean matter density contrast within the radius $R = \sigma$ is $\bar{\delta} = 1$ at the present time.

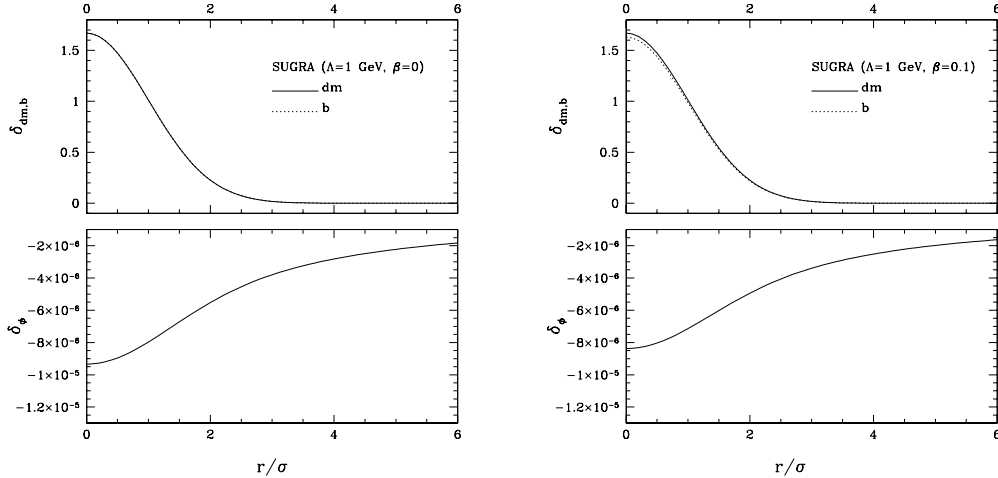


Figure 7. Same as Figure 6 but using the SUGRA potential.

Formation of DE overdensities during ϕ MDE is understood as follows. Let δw be the first order correction to the state parameter w due to the perturbation in the scalar field:

$$\delta w = \frac{1}{\bar{\rho}_\phi} (\delta P_\phi - w \delta \rho_\phi) \quad (19)$$

so that $w + \delta w$ is the perturbed state parameter inside the fluctuation. Noticing that if $\bar{\rho}_V$ is negligible with respect to $\bar{\rho}_k$, yielding $w \sim 1$, and $\delta \rho_k > 0$, $\delta \rho_V < 0$ as previously observed, we will also have that $\bar{\rho}_k + \delta \rho_k \gg \bar{\rho}_V + \delta \rho_V$. Therefore, $w + \delta w \sim w \sim 1$ (or $\delta w \sim 0$) and from (19) it follows $|\delta \rho_k| \gg |\delta \rho_V|$.

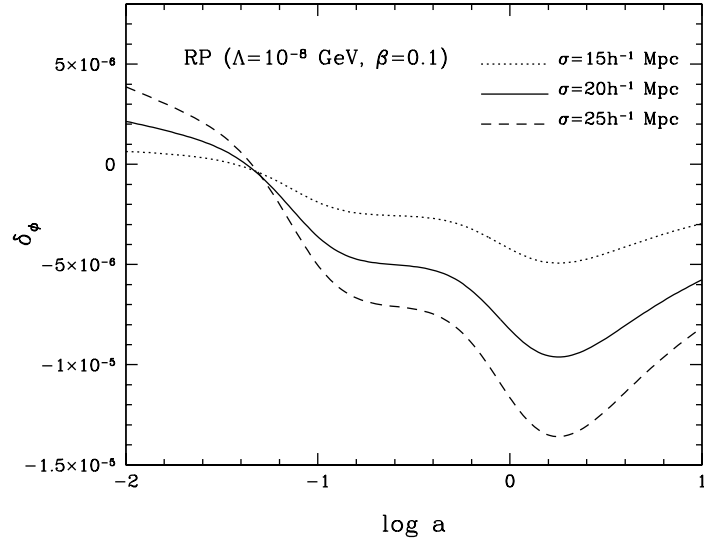


Figure 8. Evolution of the DE density contrast, δ_ϕ , at the center of a spherical matter overdensity in coupled RP models when different scales σ are considered. Perturbations on shorter scales are suppressed.

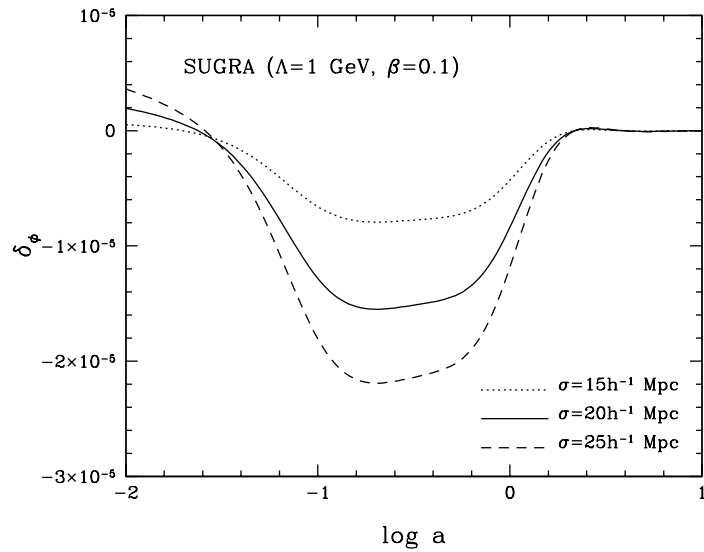


Figure 9. Same as Figure 8 but using SUGRA potential.

After ϕ MDE, δ_ϕ falls off to negative values resuming the same qualitative behavior as in the uncoupled case. Notice that fluctuation amplitudes decrease when increasing the coupling strength. In fact, it shortens the period between the end of ϕ MDE and DE dominance so that less time will be left for the perturbation growth.

As soon as DE becomes the dominant component, $|\delta_\phi|$ starts to decrease to zero as the Universe approaches the de Sitter attractor.

Figure 5 shows the mean density contrast of DM and baryons, $\bar{\delta}_{dm,b}$, within the radius $r = \sigma$, as a function of the scale factor. Results are given for the SUGRA model, only slightly differences occur when considering different cases. As expected, growth of matter perturbations is suppressed once DE dominates the cosmic expansion. Also, notice how coupling introduces a bias between baryons and DM causing fluctuations to grow at different rates.

Mean density contrasts, $\bar{\delta}_{dm,b}$, are easily obtained from (16) as the assumed initial gaussian shape of matter perturbations is kept during their evolution. This is confirmed by numerical results and shown in the top panels of Figures (6) and (7) which display the density profiles of DM and baryons for different models at the present time. Density profiles of DE are then shown in the bottom panels of the same figures.

Figures (8) and (9) compare the growth of DE perturbations, when different scales are considered showing how perturbations on shorter scales are suppressed.

So far, we have considered the behavior of DE perturbations in the presence of matter overdensities. We now look at what happens in the presence of matter underdensities or voids. It is not surprising to expect that DE perturbations behave in an opposite fashion given that local voids increase the local value of H and consequently $\delta\phi, \dot{\delta}\phi < 0$. This is confirmed by the Figures (10), (11) and (12) which display the time evolution of δ_ϕ for matter density contrasts and scales typical of voids and supervoids (see next section). Although different models are considered, our results are quite general. We find the largest DE inhomogeneities ($|\delta_\phi| \sim \mathcal{O}(10^{-4} - 10^{-3})$) to be associated with objects on very large scale ($\sim 300h^{-1}$ Mpc) which existence was recently postulated in [25] and [26]. On typical supervoid scales we obtain $|\delta_\phi| \sim \mathcal{O}(10^{-5} - 10^{-4})$ while we find even smaller $|\delta_\phi| \sim \mathcal{O}(10^{-6} - 10^{-5})$ in the presence of voids and supercluster.

4. Summary and conclusions

Unlike cosmological constant models (Λ CDM), models of DE which have a dynamical nature yield a varying state parameter $w(a)$. Although current limits on w are consistent with a cosmological constant ($w = -1 \pm 0.1$, [20]), detecting either $w \neq -1$ or its time variation ($dw/da \neq 0$), would provide a crucial support for dynamical DE. Nevertheless, many models of dynamical DE predict no substantial deviation from $w = -1$ in the late time evolution providing a background cosmology very closed to that of Λ CDM.

Anyway, dynamical DE stops to mimic a cosmological constant when one deals with their clustering properties as dynamical DE is expected not to be perfectly homogeneous. Clustering properties of dynamical DE in the vicinity of matter inhomogeneities was

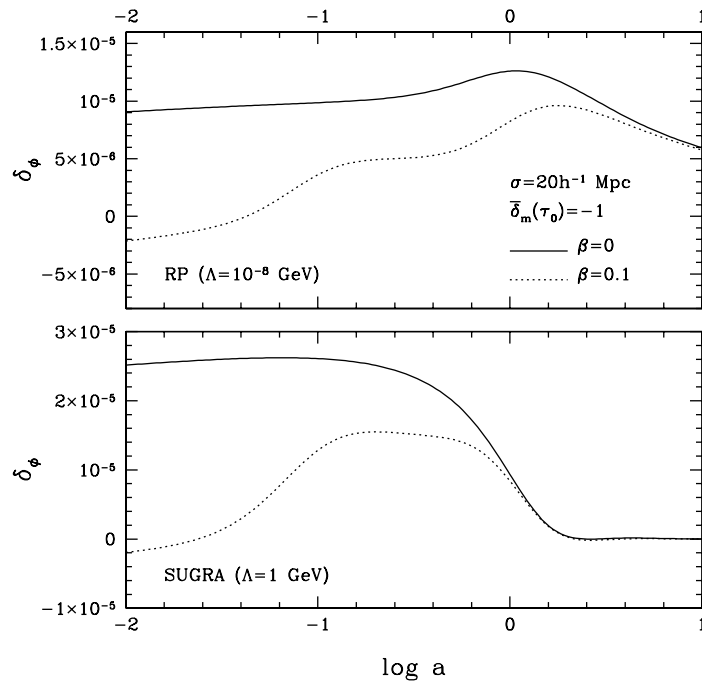


Figure 10. Evolution of the DE density contrast, δ_ϕ , at the center of a spherical matter underdensity in RP (top) and SUGRA (bottom) models. Plots are given for the comoving scale $\sigma = 20h^{-1}$ Mpc. The mean matter density contrast within the radius $R = \sigma$ is $\bar{\delta} = -1$ at the present time. Such features are typical of matter voids.

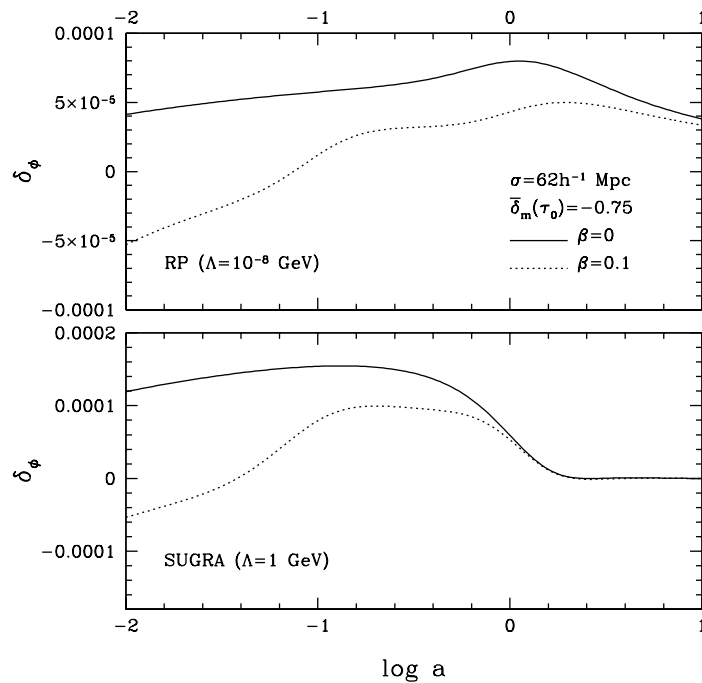


Figure 11. Same as Figure 10 but for $\sigma = 62h^{-1}$ and $\bar{\delta} = -0.75$. Such values has been estimated for the Boötes supervoid (see text).

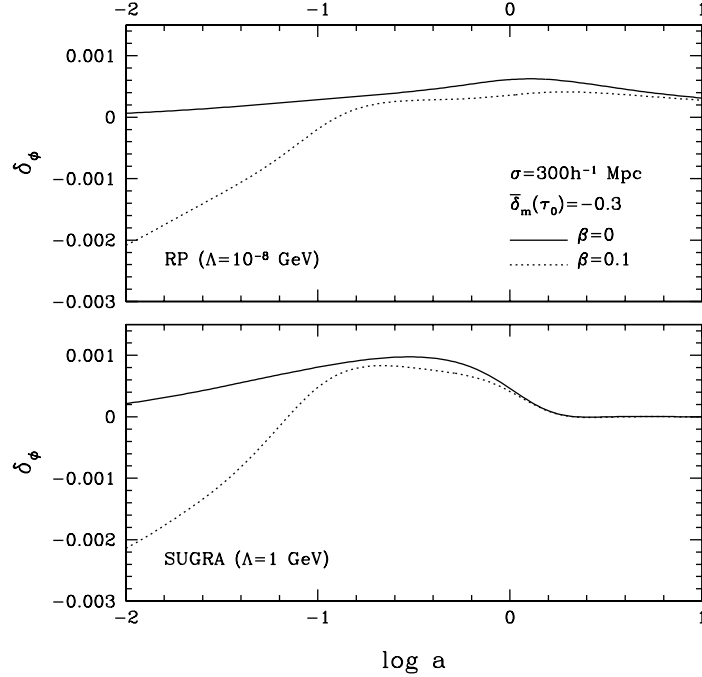


Figure 12. Same as Figure 10 but for $\sigma = 300h^{-1}$ and $\bar{\delta} = -0.3$. The existence of matter voids with these properties has been recently postulated to explain the observed large angle anomalies of the CMB (see text).

recently studied by Dutta & Maor [9] and Mota et al [10] using two different approaches. While the formers face the problem by numerical methods evolving the linearized perturbations equations, the latter use an analytical approach which permitted them to extend the analysis even to the nonlinear regime.

One of the most striking results of the above works is that DE tends to form voids in correspondence of linear matter overdensities. However, discrepancies between quantitative results are found. When $\delta_m \sim \mathcal{O}(1)$, Dutta & Maor [9] find significant void amplitudes, $|\delta_\phi| \sim \mathcal{O}(10^{-2})$, which could be relevant to observations, e.g. on supercluster scales. On the other hand, Mota et al [10] report $|\delta_\phi| \sim \mathcal{O}(10^{-5})$.

In both the works, DE is modeled as a self-interacting scalar field minimally coupled to matter and gravity.

In this paper we have extended the analysis to a wider class of DE scalar fields admitting tracker solutions also allowing for a possible coupling between DM and DE. By using the same numerical approach as Dutta & Maor [9], we have studied the clustering properties of DE in presence of linear matter inhomogeneities on supercluster, void and supervoid scales.

Superclusters are the largest known gravitationally bound massive structures with typical radii of about $10 - 25h^{-1}$ Mpc and mean density contrasts $\bar{\delta} \sim 1 - 15$. Typical examples are the local supercluster (LSC), of which our galaxy is a part, and the Shapley

supercluster (SSC) which is ~ 650 Mly from us. The LSC has a mean overdensity of $\bar{\delta}_m \sim 2 - 3$ over a scale $\sim 15h^{-1}$ Mpc [21] while the SSC has been found to have an overdensity of $\bar{\delta}_m \sim 10.3$ over a scale of $10.1h^{-1}$ Mpc [22]. In addition to matter overdensities, Universe contains voids of matter typically having radii similar to superclusters or even larger (supervoids). Data from 2dFGRS are consistent with voids having average radii of $\sim 15h^{-1}$ Mpc and average mean density contrast $\bar{\delta}_m \sim -0.93$ [23]. An example of a supervoid is the Boötes void found to be roughly spherical with radius of $\sim 62h^{-1}$ Mpc [24] and a mean density contrast estimated to be $-0.8 < \bar{\delta}_m < -0.66$.

Recently, the possibility that extremely large voids might exist with radii of $\sim 100 - 300$ Mpc, has been considered. In particular in [25] it is shown that the Integrated Sachs Wolfe (ISW) effect due to a void with radius $\sim 200 - 300$ Mpc and $\bar{\delta}_m \sim -0.3$ would be observed as a cold spot in the CMB radiation explaining the observed large angle CMB anomalies (see also [26] for a similar conclusion). According to our results (and those of Mota et al [10] as well) such extremely large objects would correspond to the largest DE overdensities.

We conclude summarizing our main results concerning the behavior of DE perturbations in the vicinity of matter inhomogeneities. In the presence of matter overdensities we find that:

- (i) DE tends to form voids if no coupling to DM is present
- (ii) in coupled models, DE overdensities form during ϕ MDE. After this stage δ_ϕ becomes negative resuming the same behavior as in the uncoupled case.

If matter underdensities are considered, DE perturbations behave in the opposite fashion. From our analysis we obtain $|\delta_\phi| \sim \mathcal{O}(10^{-6} - 10^{-5})$ for voids and supercluster, $|\delta_\phi| \sim \mathcal{O}(10^{-5} - 10^{-4})$ for supervoids and if extremely large voids exist $|\delta_\phi| \sim \mathcal{O}(10^{-4} - 10^{-3})$. Our results are consistent with those of Mota et al [10] indicating that if DE is described by a scalar field, either uncoupled or coupled with DM, it would be almost homogeneous on sub-horizon scales above that of galaxy clusters.

Further, in general we have:

- (i) within matter inhomogeneities DE can form voids as well as overdensities. However, the behavior of δ_ϕ is mainly related to how the background DE energy density evolves rather than to whether a matter fluctuation is an overdensity or an underdensity
- (ii) DE perturbation growth is sensitive to the scale considered. On shorter scales perturbations are suppressed
- (iii) accelerated expansion yields a suppression of DE inhomogeneities, i.e $|\delta_\phi|$ decreases to zero as the universe approaches the de Sitter attractor.

We have shown in the previous section that $|\delta_\phi|$ decreases at the increasing of the coupling strength β when supercluster and void scales are considered. According to the first of the above claims, the fluctuation suppression due to the coupling is then to impute to the fact that perturbations grow on horseback of two distinct evolutionary phases of

the scalar field, namely ϕ MDE and usual tracking phase in matter era, changing their sign. It would be interesting to ascertain whether such effect also holds when dealing with nonlinear matter collapse, e.g. on galaxy cluster scales. If so, very small DE perturbations are expected, at most not larger than what found by Mota et al [10] when considering nonlinear scales in uncoupled DE models, i.e. $\delta_\phi \sim \mathcal{O}(10^{-5})$. This would be a quite unexpected result since it seems natural to believe that infalling matter, when coupled to DE, will drag along DE permitting larger DE perturbations.

Suppression of DE perturbations due to the coupling is however strictly true only after ϕ MDE if larger scales are considered. During ϕ MDE, DE fluctuations are only marginally suppressed on supervoid scales, while they can be as large as matter fluctuations on extremely large scales ($\sim 200 - 300$ Mpc). Figure 12 indicates $\delta_\phi \sim \delta_m$ at $z \sim 100$ and even larger values are expected for higher z . suggesting the possibility that DE clustering might be detected through the ISW effect.

As already observed in [27], an interaction between DM and DE changes both the scaling of the DM energy density and the growth rate of matter perturbations affecting the time evolution of the metric potentials and, consequently, the ISW effect. Our results point out that, in coupled cosmologies, a further contribution to ISW effect can arise during ϕ MDE from DE perturbations associated with very large voids of matter.

Further investigations on this last point and the behavior of DE in the presence of nonlinear matter inhomogeneities are left to future works.

Acknowledgments

I wish to thank A. Gardini, for useful hints and discussions. I am also grateful to J.R. Kristiansen for reading the manuscript and pointing out some corrections. This work is supported by the Research Council of Norway, project number 162830.

Appendix A.

In a spacetime described by the metric (4):

$$ds^2 = -dt^2 + \mathcal{U}(t, r)dr^2 + \mathcal{V}(t, r) \left(d\theta^2 + \sin^2 \theta d\varphi^2 \right) \quad (\text{A.1})$$

the Einstein's equations take the form:

$$\frac{1}{2} \frac{\ddot{\mathcal{U}}}{\mathcal{U}} + \frac{1}{2} \frac{\dot{\mathcal{U}} \dot{\mathcal{V}}}{\mathcal{U} \mathcal{V}} - \frac{1}{4} \frac{\dot{\mathcal{U}}^2}{\mathcal{U}^2} + \frac{1}{\mathcal{U}} \left(\frac{1}{2} \frac{\mathcal{U}' \mathcal{V}'}{\mathcal{U} \mathcal{V}} + \frac{1}{2} \frac{\mathcal{V}''}{\mathcal{V}^2} - \frac{\mathcal{V}''}{\mathcal{V}} \right) = -4\pi G \left(T_0^0 - T_1^1 + 2T_2^2 \right) \quad (\text{A.2})$$

$$\frac{1}{2} \frac{\ddot{\mathcal{V}}}{\mathcal{V}} + \frac{1}{4} \frac{\dot{\mathcal{U}} \dot{\mathcal{V}}}{\mathcal{U} \mathcal{V}} + \frac{1}{\mathcal{V}} + \frac{1}{2\mathcal{U}} \left(\frac{1}{2} \frac{\mathcal{U}' \mathcal{V}'}{\mathcal{U} \mathcal{V}} - \frac{\mathcal{V}''}{\mathcal{V}} \right) = -4\pi G \left(T_0^0 + T_1^1 \right) \quad (\text{A.3})$$

$$\frac{1}{2} \frac{\dot{\mathcal{U}} \dot{\mathcal{V}}}{\mathcal{U} \mathcal{V}} + \frac{1}{4} \frac{\dot{\mathcal{V}}^2}{\mathcal{V}^2} + \frac{1}{\mathcal{V}} + \frac{1}{\mathcal{U}} \left(\frac{1}{2} \frac{\mathcal{U}' \mathcal{V}'}{\mathcal{U} \mathcal{V}} + \frac{1}{4} \frac{\mathcal{V}''}{\mathcal{V}^2} - \frac{\mathcal{V}''}{\mathcal{V}} \right) = -8\pi G T_0^0 \quad (\text{A.4})$$

$$\frac{1}{2} \frac{\dot{\mathcal{U}} \mathcal{V}'}{\mathcal{U} \mathcal{V}} + \frac{1}{2} \frac{\dot{\mathcal{V}} \mathcal{V}'}{\mathcal{V} \mathcal{V}} - \frac{\dot{\mathcal{V}}'}{\mathcal{V}} = -8\pi G T_1^1 \quad (\text{A.5})$$

while from (1) it follows:

$$\ddot{\phi} + \left(\frac{\dot{\mathcal{V}}}{\mathcal{V}} + \frac{1}{2} \frac{\dot{\mathcal{U}}}{\mathcal{U}} \right) \dot{\phi} - \frac{1}{\mathcal{U}} \left[\left(\frac{\mathcal{V}'}{\mathcal{V}} - \frac{1}{2} \frac{\mathcal{U}'}{\mathcal{U}} \right) \phi' + \phi'' \right] + \frac{dV}{d\phi} = C \rho_{dm} \quad (\text{A.6})$$

$$\dot{\rho}_{dm} + \left[\frac{\dot{\mathcal{V}}}{\mathcal{V}} + \frac{1}{2} \frac{\dot{\mathcal{U}}}{\mathcal{U}} + \left(\frac{\mathcal{V}'}{\mathcal{V}} + \frac{1}{2} \frac{\mathcal{U}'}{\mathcal{U}} \right) v_{dm}^r + v_{dm}^{r'} \right] \rho_{dm} + \rho'_{dm} v_{dm}^r = -C \dot{\phi} \rho_{dm} \quad (\text{A.7})$$

$$\dot{v}_{dm}^r + \left(\frac{\dot{\mathcal{V}}}{\mathcal{V}} + \frac{3}{2} \frac{\dot{\mathcal{U}}}{\mathcal{U}} + \frac{\dot{\rho}_{dm}}{\rho_{dm}} \right) v_{dm}^r = C \frac{\phi'}{\mathcal{U}} \quad (\text{A.8})$$

$$\dot{\rho}_b + \left[\frac{\dot{\mathcal{V}}}{\mathcal{V}} + \frac{1}{2} \frac{\dot{\mathcal{U}}}{\mathcal{U}} + \left(\frac{\mathcal{V}'}{\mathcal{V}} + \frac{1}{2} \frac{\mathcal{U}'}{\mathcal{U}} \right) v_b^r + v_b^{r'} \right] \rho_b + \rho'_b v_b^r = 0 \quad (\text{A.9})$$

$$\dot{v}_b^r + \left(\frac{\dot{\mathcal{V}}}{\mathcal{V}} + \frac{3}{2} \frac{\dot{\mathcal{U}}}{\mathcal{U}} + \frac{\dot{\rho}_b}{\rho_b} \right) v_b^r = 0 \quad (\text{A.10})$$

Here, overdots and primes denote the derivatives with respect to t and the radial coordinate r respectively. Only radial motions are considered and terms quadratic in $v_{dm,b}^r$ has been neglected as DM and baryons are non-relativistic components.

According to (5) and (6) we decompose our variables in an homogeneous part and a perturbation. It is then straightforward to obtain the equations for the background:

$$3\mathcal{H}^2 = 8\pi G [\bar{\rho}_{dm} + \bar{\rho}_b + \bar{\rho}_\phi] \quad (\text{A.11})$$

$$\ddot{\bar{\phi}} + 3\mathcal{H}\dot{\bar{\phi}} + \bar{V}' = C\bar{\rho}_{dm} \quad (\text{A.12})$$

$$\dot{\bar{\rho}}_{dm} + 3\mathcal{H}\bar{\rho}_{dm} = -C\bar{\rho}_{dm}\dot{\bar{\phi}} \quad (\text{A.13})$$

$$\dot{\bar{\rho}}_b + 3\mathcal{H}\bar{\rho}_b = 0 \quad (\text{A.14})$$

To linear order, (A.2)–(A.5) gives the equations for the metric perturbations:

$$\ddot{\zeta} + 2H(2\dot{\zeta} + \dot{\psi}) + \frac{2}{a^2} \left(\frac{\zeta'}{r} - \frac{2\psi'}{r} - \psi'' \right) = 4\pi G (\delta\rho_{dm} + \delta\rho_b + \delta\rho_\phi - \delta P_\phi) \quad (\text{A.15})$$

$$\ddot{\psi} + H(5\dot{\psi} + \dot{\zeta}) + \frac{1}{a^2} \left(\frac{2\zeta}{r^2} - \frac{2\psi}{r^2} + \frac{\zeta'}{r} - \frac{4\psi'}{r} - \psi'' \right) = 4\pi G (\delta\rho_{dm} + \delta\rho_b + \delta\rho_\phi - \delta P_\phi) \quad (\text{A.16})$$

$$2H(\dot{\zeta} + 2\dot{\psi}) + \frac{2}{a^2} \left(\frac{\zeta}{r^2} - \frac{\psi}{r^2} + \frac{\zeta'}{r} - \frac{3\psi'}{r} - \psi'' \right) = 8\pi G (\delta\rho_{dm} + \delta\rho_b + \delta\rho_\phi) \quad (\text{A.17})$$

$$\frac{2}{r} (\dot{\zeta} - \dot{\psi}) - 2\dot{\psi}' = -8\pi G [\bar{\rho}_{dm} v_{dm}^r + \bar{\rho}_b v_b^r + (\bar{\rho}_\phi + \bar{P}_\phi) v_\phi^r] a^2 \quad (\text{A.18})$$

while perturbation equations for DE, DM and baryons follow from (A.6)–(A.10):

$$\delta\ddot{\phi} + 3H\delta\dot{\phi} - \frac{1}{a^2} \left(\delta\phi'' + \frac{2}{r}\delta\phi' \right) + \frac{d^2\bar{V}}{d\phi^2} \delta\phi + (\dot{\zeta} + 2\dot{\psi}) \dot{\phi} = C\delta\rho_{dm} \quad (\text{A.19})$$

$$\delta\dot{\rho}_{dm} + 3H\delta\rho_{dm} + (\dot{\zeta} + 2\dot{\psi}) \rho_{dm} + \left(v_{dm}^{r'} + \frac{2}{r} v_{dm}^r \right) \rho_{dm} = -C \left(\dot{\bar{\phi}} \delta\rho_{dm} + \delta\dot{\bar{\phi}} \bar{\rho}_{dm} \right) \quad (\text{A.20})$$

$$\dot{v}_{dm}^r + 2Hv_{dm}^r = C \left(\dot{\bar{\phi}} v_{dm}^r + \frac{\delta\phi'}{a^2} \right) \quad (\text{A.21})$$

$$\delta\dot{\rho}_b + 3H\delta\rho_b + (\dot{\zeta} + 2\dot{\psi}) \rho_b + \left(v_b^{r'} + \frac{2}{r} v_b^r \right) \rho_b = 0 \quad (\text{A.22})$$

$$\dot{v}_b^r + 2Hv_b^r = 0 \quad (\text{A.23})$$

Combining equations (A.15), (A.16) and (A.17) gives:

$$\left(\ddot{\zeta} + 2\ddot{\psi}\right) + 2H\left(\dot{\zeta} + 2\dot{\psi}\right) = -4\pi G\left(\delta\rho_{dm} + \delta\rho_b + \delta\rho_\phi + 3\delta P_\phi\right) \quad (\text{A.24})$$

It is clear, from the above equations, that $\chi = \dot{\zeta} + 2\dot{\psi}$ is the only combination which is relevant for the evolution equations of DE, DM and baryons perturbations.

When rewritten in terms of the conformal time τ and the variables χ , $\delta_i = \delta\rho_i/\bar{\rho}_i$ and $\theta_i = v_i^r + 2v_i^r/r$ ($i = dm, b, \phi$) equations (A.11)–(A.14) and (A.19)–(A.24) gives (9) and (8) respectively.

References

- [1] Tegmark M. et al., 2004, Phys.Rev. D69, 10350; De Bernardis et al., 2000 Nature 404, 955; Hanany S. et al, 2000, ApJ 545, L5; Halverson N.W. et al. 2002, ApJ 568, 38; Percival W.J. et al., 2002, MNRAS, 337, 1068, Riess, A.G. et al., 1998, Aj 116, 1009; Perlmutter S. et al., 1999, Apj, 517, 565
- [2] Kristiansen J. R., Elgarøy Ø., Dahle H., 2007, Phys. Rev. D75, 083510; see also Elgarøy Ø. et al., 2002, Phys. Rev. Lett. 89, 061301
- [3] La Vacca G., Bonometto S. A., Colombo L. P. L., 2008 arXiv:0810.0127; La Vacca, Kristiansen J. R., Colombo L. P. L., Mainini R., Bonometto S. A., 2009, arXiv:0902.2711, JCAP submitted; Kristiansen J. R., La Vacca, Colombo L. P. L., Mainini R., Bonometto S. A., 2009, arXiv:0902.2737, Phys.Rev.Lett. submitted
- [4] Copeland E. J., Sami M., Tsujikawa S., 2006, Int.J.Mod.Phys D15, 1753
- [5] Peebles P.J.E. & Ratra B., 2003, Rev.Mod.Phys. 75, 559
- [6] Wang L. & Steinhardt P.J., 1998, ApJ, 508, 483; Mainini R., Maccio' A., Bonometto S., 2003, New Astron. 8, 173; Mainini R., Maccio' A., Bonometto S., Klypin A., 2003, ApJ. 599, 24; Klypin A., Maccio' A., Mainini R., S.A. Bonometto, 2003, ApJ, 599, 24; Lokas E. L., Bode P., Hoffman Y., 2004, MNRAS, 349, 595; Horellou C., Berge J., 2005, MNRAS, 360, 1393
- [7] Matarrese S., Pietroni M., Schimd C., 2003, JCAP 0308, 005; Perrotta F., Matarrese S., Pietroni, Schimd C., 2004, Phys.Rev. D69, 084004 Mainini R., 2005, Phys.Rev. D72, 083514; Mainini R. & Bonometto S. A., 2006, Phys.Rev. D74, 043504; Abramo L. R., Batista R. C., Liberato L., Rosenfeld R., 2007, JCAP 11, 012; Mainini R., 2008, JCAP, 07, 003
- [8] Nunes N. J., da Silva A. C., Aghanim N., 2005, A&A 450, 899; Mota D. & van de Bruck C., 2004, A&A, 421,71; Maor I., Lahav O., 2005, JCAP 0507, 003; Wang P., 2006, ApJ 640,18; Nunes J. N. & Mota D., 2006, MNRAS 368, 75; Manera M. & Mota D., 2006, MNRAS 371, 1373;
- [9] Dutta S. & Maor I., 2007, Phys.Rev. D75, 063507
- [10] Mota D., Shaw J., Silk J., 2008, ApJ 675, 29
- [11] Maccio' A. V., Quercellini C., Mainini R., Amendola L., Bonometto S. A., 2004, Phys. Rev. D69, 123516
- [12] Amendola L. & Quercellini C., 2003, Phys. Rev. D69; Olivares G., Atrio-Barandela F., Pavon D., 2005, Phys.Rev. D71, 063523; Lee S., Liu G. & Ng K., 2006, Phys.Rev. D73, 083516; Guo Z., Ohta N. & Tsujikawa S., 2007, Phys.Rev. D76, 023508; Mainini R. & Bonometto S. A., 2007, JCAP 06,020
- [13] Amendola L., 2000, Phys.Rev. D62, 043511; Amendola L., 2004, Phys.Rev. D69, 103524
- [14] Dolag K. et al., 2004, A&A 416, 853; Olivares G., Atrio-Barandela F., Pavon D., 2006, Phys.Rev. D74, 043521
- [15] Ellis J., Kalara S., Olive K.A. & Wetterich C., 1989, Phys. Lett. B228, 264; Casas J.A., Garcia-Bellido J. & Quiros M., 1992, Class.Quant.Grav. 9, 1371; Wetterich C., 1995, A&A 301, 321; Anderson G.W. & Carroll S.M., Procs. of "COSMO-97, First International Workshop on Particle Physics and the Early Universe", Ambleside, England, September 15-19, 1997, astro-ph/9711288; Bartolo N. & Pietroni M., 2000, Phys.Rev. D61, 023518; Gasperini M., Piazza F. & Veneziano

- G., 2002, Phys.Rev. D65, 023508; Mangano G., Miele G., Pettorino V., 2003, Mod.Phys.Lett. A18, 831 Pietroni M., 2003, Phys.Rev D67, 103523; Chimento L.P., Jakubi A.S., Pavon D. & Zimdahl W., 2003, Phys.Rev D67, 083513; Rhodes C.S., van de Bruck C, Brax P., & Davis A.C., 2003, Phys.Rev. D68, 083511; Mainini R. & Bonometto S.A., 2004, Phys.Rev.Lett., 93, 121301; Khoury J. & Weltman A., 2004, Phys.Rev. D69, 044026; Farrar G.R. & Peebles P.J.E., 2004, ApJ 604, 1; Gromov A., Baryshev Y. & Teerikorpi P., 2004, A&A, 415, 813; Fuzfa A. & Alimi J.M., 2007, Phys.Rev. D75, 123007; Chimento L. & Forte M., 2008, Phys.Lett.B, 666, 205
- [16] See for example, Weinberg S., 1972 *Gravitation and Cosmology: Principles and Applications of the General Theory of Relativity*, Wiley
- [17] Ratra B. & Peebles P.J.E., 1988, Phys.Rev D37, 3406; Brax P., Martin J., Riazuelo A., 2000, Phys.Rev. D62, 103505
- [18] Colombo L.P.L. & Gervasi M., 2006, JCAP 10,001; Mainini R., Colombo L.P.L, Bonometto S.A., 2005, ApJ. 632, 691
- [19] Barreiro T., Copeland E.J., Nunes N.J., 2000, Phys.Rev. D61, 127301
- [20] Riess et al, 2007, ApJ, 659, 98
- [21] Hoffman Y., 1986, ApJ, 308, 493; Tully R.B., 1982, ApJ, 257, 389
- [22] Bardelli S., Zucca E., Zamorani G., Moscardini L., Scaramella R., 2000, MNRAS, 312, 540
- [23] Hoyle F. & Vogeley M.S., 2004, ApJ, 607, 751; Bolejko K., Krasinski A., Hellaby C., 2005, MNRAS, 362, 213
- [24] Kirschner R.P., Oemler A., Schechter P.L., Shectman, 1987, ApJ, 314, 493
- [25] Inoue K.T. & Silk J., 2007, Apj, 664, 650
- [26] Rudnick L., Brown S., Williams L.R., 2007, ApJ 671, 40
- [27] German Olivares G., Atrio-Brandela F., Pavon D., 2008, Phys.Rev. D77, 103520 Schaefer B.M., 2008, MNRAS, 388, 1403